

Some physical organic aspects of salicylaldehydes oximes, a theoretical study

Tareq Irshaidat *

Department of Chemistry, College of Sciences, Al-Hussein Bin Talal University, Ma'an, Jordan

Received 17 October 2007; revised 12 November 2007; accepted 22 November 2007

Abstract

Molecular structures of two oximes derived from salicylaldehyde and 2-hydroxynaphthaldehyde were studied using the B3LYP functional and the basis set 6-31G(d). This study discusses the electron/proton localization in the two oximes qualitatively based on the calculated infrared frequencies, two types of atomic charges, and the aromaticity index HOMA.

© 2007 Elsevier Ltd. All rights reserved.

1. Introduction

Imines derived from salicylaldehyde and 2-hydroxynaphthaldehyde are typical examples of photochromic and thermochromic compounds that continue to attract wide interest because of their technological applications.^{1–3} Photochromism and thermochromism of these compounds occur due to their ability to undergo proton and electron transfer from one atom through the conjugated system, that is, reversible tautomerism between enol and keto forms caused by electromagnetic radiation or heat. In the case of salicylideneanilines, photochromism and thermochromism in the crystalline state have been considered as mutually exclusive phenomena.^{4–6}

Factors affecting tautomerism in a wide range of derivatives have been studied. The existence of the imine group in the same plane of the phenyl or the naphthyl groups is an important factor in H-transfer. However, overall molecular planarity is not necessary.⁷ It has been postulated that a crucial factor for facile H-transfer resulting in thermochromism is the electron density on the imine N-atom.⁸ Besides the amine part of the molecules, the nature of the substituent group(s) on the salicylidene moiety is a poten-

tial factor that can influence the electron distribution of the system and can drive the equilibrium from the enol towards the keto form.

Oximes of salicylaldehyde and 2-hydroxynaphthaldehyde are stable compounds and can be prepared easily by a simple condensation procedure. The stability and simplicity of the preparative procedure are two desired properties of the applied materials. Unfortunately, these molecules do not exhibit any photochromic or thermochromic behavior, which is attributed to electron–proton localization. In this computational study, we intended to shed light on the two elements of this issue separately. Diagnosis of the electron localization was achieved by calculating the atomic charges (Mulliken and natural population analysis charges) and the

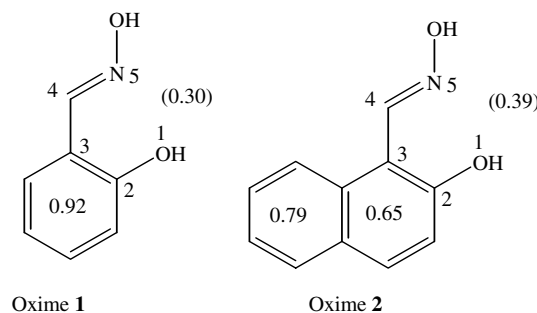


Fig. 1. Structures of the oximes derived from salicylaldehyde and 2-hydroxy-1-naphthaldehyde and the calculated HOMA values.^{9–11}

* Tel.: +962 799514989; fax: +962 32179050.
E-mail address: tirshaidat@yahoo.com

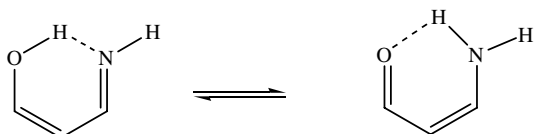


Fig. 2. The simplest OCCCN tautomerism system.

aromaticity index harmonic oscillator measure of aromaticity (HOMA).^{9–11} Proton localization was characterized qualitatively using the calculated infrared frequencies. In addition to the two oximes **1** and **2** (Fig. 1), the compounds naphthalene (**3**), phenanthrene (**4**), isoquinoline (**5**), and 1,2-benzoxazole (**6**) (Fig. 4) have been selected to exhibit possible variations in HOMA values in different aromatic systems. Another purpose for this study is to develop a computational procedure for studying larger systems within shorter times compared to previous recommendations with acceptable accuracy.

2. Computational method

The aromaticity index HOMA^{9–11} is a method that takes advantage of the bond lengths of the interesting molecular segment. For example, if we consider the conjugated cyclic system of the formula C₆H₆, the value HOMA = 0 represents the system with fully localized double bonds which is known as the Kekule' structure while HOMA = 1 is for the fully delocalized system, the known benzene ring. Values of HOMA less than unity and greater than zero are the most common. HOMA is useful for various systems and bond types.^{9–11}

Gas phase calculations at the B3LYP/6-31G(d)^{12–14} level of theory were applied to all the structures in Figures 1 and 3. All calculations were performed using the GAUSSIAN 03

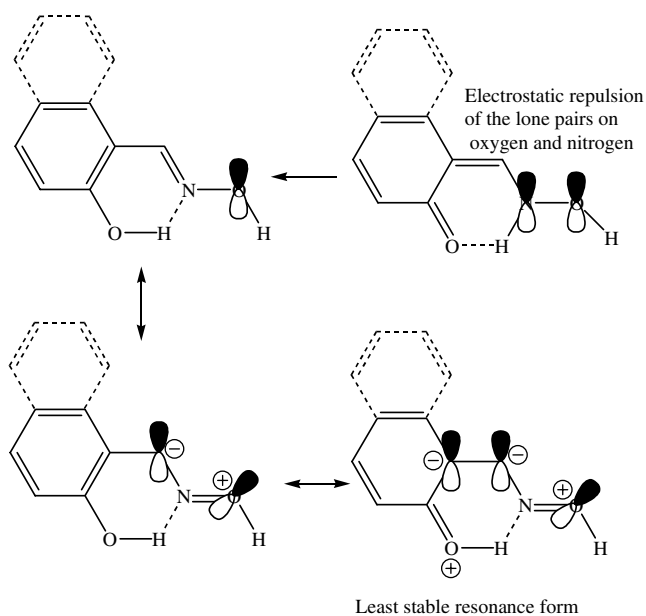


Fig. 3. Illustration of the dominance of the enol form based on electrostatic interactions.

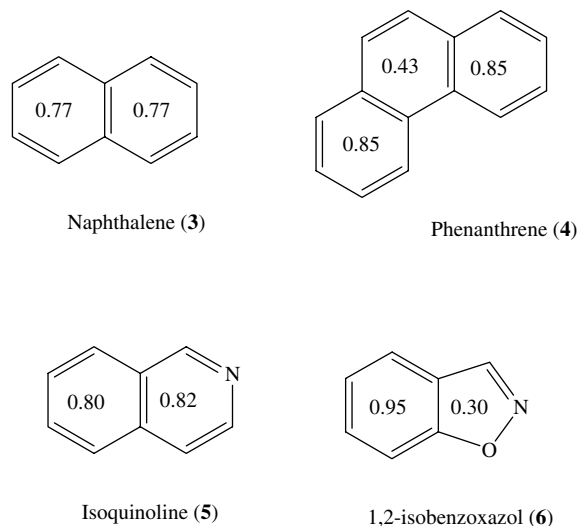


Fig. 4. HOMA values for selected polycyclic systems.

series of programs.¹⁵ The basis set, 6-311+G(d,p)¹⁶ was recommended by Wiberg¹⁷ as leading to satisfactory structures (the estimated HOMA is 0.99 for benzene). However, 6-31G(d) is another good basis set and provides a very close HOMA value for benzene which is equal to 0.98. Natural population analysis (NPA) charges¹⁸ can be calculated for an optimized geometry in GAUSSIAN 03 by specifying the keyword "POP=NPA" in the input file.¹⁵ Mulliken charges¹⁹ were obtained from the default output file of the calculations; the software GAUSSIAN 03 calculates these charges for optimized geometry. After performing frequency calculations both thermodynamic parameters and infrared vibrations were obtained. The frequencies presented were selected to represent best the stretching vibrations of the indicated diatomic groups (Table 2). The simplest OCCCN system (Fig. 2) was used to compare energy differences (Table 1) using different basis sets.

3. Results and discussion

Attempts to optimize the keto form for structures **1** and **2** always gave back the enol–imine form (structures **1** and **2**) which indicates that the keto–enamine form is highly unfavorable and the proton of the OCCCN segment prefers bonding to oxygen.

Table 1
HOMA and ΔE (in kcal/mol) from different basis sets for the simplest tautomerizing system OCCCN

Basis set	HOMA	ΔE
6-31G(d)	0.81	–8.96
6-31G(d,p)	0.81	–7.48
6-311G(d,3p)	0.81	–7.46
6-311+G(d,p)	0.80	–8.14
6-311++G(d,p)	0.79	–8.15
6-311+G(d,p) ^a	—	–8.18 ^a

^a Single point calculation of ΔE on the geometry optimized by the basis set 6-31G(d).

4. Evaluation of basis sets

The simplest tautomerizing system OCCCN as it appears in Figure 2 has been used to evaluate different basis sets using the B3LYP functional. The basis set 6-311+G(d,p) was recommended for similar cases.¹⁷ The HOMA values are very close to each other. Basis sets 6-31G(d), 6-31G(d,p), and 6-311G(d,3p) gave identical HOMA values (0.81). Increasing the size of the basis set and adding polarization function(s) on the hydrogen atoms did not affect the values of HOMA. Addition of diffuse function(s) started to affect the value but the difference was not that significant. The basis set 6-311++G(d,p) changed the value by 0.02 from the value calculated by 6-31G(d). Based on HOMA calculations, the basis set 6-31G(d) appears to be more practical for this type of comparative study. ΔE values support the keto-enamine as the major form. The largest value (8.96 kcal/mol) was obtained from the basis set 6-31G(d). The difference between this value and the value obtained by the basis set 6-311+G(d,p) (8.14 kcal/mol) is 0.82 kcal/mol. When we take into consideration how favorable the keto-enamine form is based on all five basis sets it is possible to accept the difference 0.82 kcal/mol and consider it negligible. Again, and based on the ΔE values, the basis set 6-31G(d) is considered suitable for this type of calculation in which one form is clearly more favorable than the other. For smaller ΔE values, single point calculations using the basis set 6-311+G(d,p) to calculate the energy using the geometry optimized by the basis set 6-31G(d) should give very close ΔE values to that for calculations using 6-311+G(d,p), as in Table 1.

5. IR frequencies

Previously, a resonance assisted hydrogen bonding (RAHB) model was proposed in 1989²⁰ to account for the abnormally strong intramolecular O–H···O bond occurring in β -diketone enols. From an empirical point of view, this was unambiguously identified by the strict intercorrelation between hydrogen bond strength and the π -delocalization of the short conjugated chain linking the increased strength of H-bond and enhanced π -delocalization by the use of a number of bonding models.^{21–23}

Table 2 presents the most important stretching frequencies in cm^{-1} for C–O, C=N, and O–H of the enol forms of **1** and **2**. These frequencies were selected based on observing the vibrational modes of each structure. Intensities are not reported and the emphasis is on the relative energies of these

Table 2
Selected infrared frequencies (cm^{-1}) for oximes **1** and **2**

Structure	Enol–oxime forms		
	C–O	C=N	O–H
1	1324	1703	3420
2	1326	1693	3337

vibrations not to their absolute values. The differences in C–O stretching frequencies are not fully understood at this point. The value of the O–H stretching frequency of **1** (3420 cm^{-1}) is greater than that for **2** (3337 cm^{-1}). This indicates that the O–H bond in **2** is weaker than that in **1**. In these systems (O–H···N), when O–H becomes weaker H···N becomes stronger. Consequently and based on this principle, oxime **2** has stronger H···N bonds and oxygen has less localization of the electron density. In other words, we can say that in oxime **2** there is less electron density (electron)–proton coupling. Further support to this argument comes from the C=N stretching frequencies. The stretching frequency of C=N in **2** (1693 cm^{-1}) is less than that for **1** (1703 cm^{-1}) indicating weaker C=N bonding and more delocalization of the OCCCN segment for **2**. This observation is completely consistent with the conclusion drawn from the calculated O–H frequencies. This comparative approach can be useful in evaluating localization of electron density in other similar systems.

6. Atomic charges

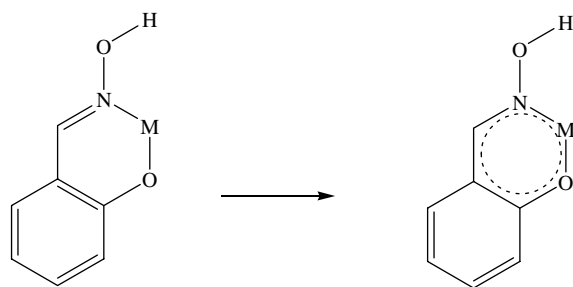
Despite its known deficiencies, the Mulliken population analysis is still widely used due to its simplicity. NPA is a more refined wave function-based method that solves most of the problems of the Mulliken scheme by construction of a more appropriate set of (natural) atomic basis functions.

The calculation of atomic charges plays an important role in the application of quantum chemical calculations to molecular systems. They are important in the qualitative rationalization of organic and inorganic reactivities.^{24–26} Table 3 presents two types of computed atomic charges for the OCCCN unit in oximes **1** and **2**; the Mulliken charges (MC) and the natural population analysis (NPA) charges (NC). In general, both MC and NC show significant similarity to each other on the atomic charges of the five atoms. Oxygen carries a negative charge in the two structures. Nitrogen carries a negative charge too, but smaller than the values for oxygen. The electronegativity of both explains the differences.

NPA charges lead to calculated values for C3 more consistent with the expected resonance in the segment O1–C2–C3 (Fig. 3). C4 appears to be nearly neutral which means that the imine group is not a powerful electron withdrawing group and, therefore, explains why the keto-enamine forms are not favorable in these cases. In other words,

Table 3
Mulliken and NPA charges for the segment OCCCN

Structure	Atoms				
	1 (O)	2 (C)	3 (C)	4 (C)	5 (N)
<i>Mulliken charges</i>					
1	−0.653	0.304	0.099	0.101	−0.271
2	−0.649	0.298	0.020	0.118	−0.290
<i>NPA charges</i>					
1	−0.690	0.372	−0.189	0.047	−0.211
2	−0.686	0.385	−0.182	0.049	−0.218



M: Li, Na, BeH, MgH, BH₂, and AlH₂

Fig. 5. The general structure for adducts of oxime **1**.

the hydroxyphenyl- and hydroxynaphthyl-groups do not feel the electronic effect of the imine group thereby favoring the aromatic forms (the enol–imine tautomer).

7. HOMA calculations for compounds **1**, **2**, **3**, **4**, **5**, and **6**

The results for compounds **3**, **4**, **5**, and **6** will be discussed first. Naphthalene (**3**) is a symmetric compound with no heteroatom which makes both rings equivalent, as indicated by the calculated HOMA value (0.77) for both rings. This value is less than unity meaning there is partial localization of the double bonds. The symmetry in phenanthrene (**4**) is different and does not imply that the three rings are identical. The middle ring is different electronically; we see more localization in the middle ring (HOMA = 0.43) with respect to the terminal rings (HOMA = 0.85). This is known for conjugated systems; the conjugation becomes less effective in keeping perfect delocalized bonds as the number of double bonds increases. Isoquinoline (**5**) shows slightly more delocalization than in naphthalene. The benzo-ring is slightly less aromatic than the heteroatom ring; 0.80 versus 0.82, respectively. Nitrogen in isoquinoline increased the aromatic nature for both rings compared to naphthalene. The electronegativity of nitrogen and similarity in size to carbon are two important factors in this difference. Compound **6** shows an unusual increase in the HOMA value for the phenyl ring (0.95) compared to naphthalene and a dramatic decrease for the heteroatom ring (0.30). The bond lengths in the phenyl ring of **6** are similar to each other but the C–O bond in the heteroatom ring suffers from considerable localization and appears as a conjugated single bond (1.355 Å) compared to the literature value²⁷ (1.367 Å). The same is true for the N–O bond; 1.412 Å, while the literature value for the single bond²⁷ is 1.415 Å. Qualitatively, these two single bonds can be attributed to the absence of effective overlap between the oxygen lone pair and the neighboring p-orbitals that exist at lower energy levels. In general, geometry optimization using 6-31G(d) produced results in complete agreement with the experimental data available for these known polycyclic systems.

Compound **1** is very similar to compound **6** with high delocalization in the phenyl ring (0.92) and considerable

localization in the OCCCN unit (0.30). The bond length of C3–C4 (1.456 Å) (according to the numbering system appearing in Fig. 1) in both structures indicates a conjugated single bond. In addition, the C–O bond in both is nearly 1.350 Å in length. Compound **2** has HOMA values of 0.79, 0.65, and 0.39. This is another similarity which shows the effect of the OH substituent, one ring has smaller HOMA values (0.65) compared to the other ring (0.79). The increase in the number of double bonds compared to **1** is the reason behind the decrease in HOMA values in **2**, a case similar to that for benzene and naphthalene.

On the other hand, replacement of hydrogen by Li, Na, MgH, BeH, AlH₂, BH₂ in **1** (Fig. 5) enhanced the HOMA values for the OCCCN segment; Li: 0.56; Na: 0.53; BeH: 0.59; MgH: 0.42; BH₂: 0.57; AlH₂: 0.57. It is obvious that chelation is essential for this change in which the OCCCN becomes quasi-aromatic. This change in HOMA values from oxime **1** to the six adducts gives a qualitative description for the proton and electron localization in **1**. Another way to describe the oximes is by saying there is proton–electron coupling. In qualitative analysis, decreasing the proton–electron coupling makes the electron attachment weaker and, in principle, should decrease the HOMO–LUMO gap and make the molecule a better electron conductor at the molecular level. Calculating the gap energy for **1** and the six adducts gave the following values in eV: oxime **1**: 4.65; Li: 4.05; Na: 3.02; MgH: 4.11; BeH: 4.30; AlH₂: 4.06; BH₂: 3.73. In general, the six adducts have gap energy values less than in oxime **1**.

Thermochromism and photochromism are two phenomena caused by interaction between electromagnetic radiation and the conjugated system. As a result, replacement of hydrogen by a different positively charged species shows the potential to alter the electronic, photochromic, and thermochromic properties of oximes making this change a new approach in designing and building new molecular materials based on the idea of ‘electron-decoupling/delocalization’.²⁸

In conclusion, we have shown that infrared stretching frequencies for O–H and C=N groups can be used to establish reasonable qualitative comparison for the electronic delocalization using the basis set 6-31G(d). NPA charges provided values more consistent with general chemical intuition. We found that the resonance that may exist in C=N–OH is important in decreasing the charge density on C4 making it nearly neutral which decreased its overlap with the segment O1–C2–C3 and therefore localized the electron density. On the other hand, HOMA calculations showed that replacement of the proton with other unipositively charged species activated the quasi-aromatic behavior as a result of a chelation type of effect. Based on the overall analysis of the two oximes in this study, they represent non-classical examples for proton/electron localization compared to Schiff bases derived from salicylaldehyde and 2-hydroxynaphthaldehyde.

Acknowledgment

The calculations were performed using the computational chemistry facilities at New Mexico State University, special thanks to Dr. H. Wang.

References and notes

1. Hadjoudis, E.; Mavridis, I. M. *Chem. Soc. Rev.* **2004**, *33*, 579.
2. Feringa, B. L.; Jager, W. F.; deLange, B. *Tetrahedron* **1993**, *37*, 8267.
3. Amimoto, K.; Kawato, T. *J. Photochem. Photobiol. C: Photochem. Rev.* **2005**, *6*, 207–226.
4. Cohen, M. D.; Schmidt, G. M. J. *J. Phys. Chem.* **1962**, *66*, 2442.
5. Bregman, J.; Leiserowitz, L.; Osaki, K. *J. Chem. Soc.* **1964**, 2086.
6. Bregman, J.; Leiserowitz, L.; Schmidt, G. M. J. *J. Chem. Soc.* **1964**, 2068.
7. Hadjoudis, E.; Vittorakis, M.; Moustakali-Mavridis, I. *Tetrahedron* **1987**, *43*, 1345.
8. Hadjoudis, E. Tautomerism by hydrogen transfer in anils. In *Photochromism: Molecules and Systems*; Durr, H., Bouas-Laurent, H., Eds.; Elsevier: Amsterdam, 1990; p 685; and references cited therein.
9. Kruszewski, J.; Krygowski, T. M. *Tetrahedron Lett.* **1972**, *36*, 3839–3842.
10. Krygowski, T. M. *J. Chem. Inf. Comput. Sci.* **1993**, *33*, 70–78.
11. Krygowski, T. M.; Cyran'ski, M. K. *Chem. Rev.* **2001**, *101*, 1385–1419.
12. Becke, A. D. *J. Chem. Phys.* **1992**, *96*, 2155; Becke, A. D. *J. Chem. Phys.* **1993**, *98*, 5648.
13. Lee, C.; Yang, W.; Parr, R. G. *Phys. Rev. B* **1988**, *37*, 785.
14. Hehre, W. J.; Ditchfield, R.; Pople, J. A. *J. Chem. Phys.* **1972**, *56*, 2257.
15. Frisch, M. J.; Trucks, G. W.; Schlegel, H. B.; Scuseria, G. E.; Robb, M. A.; Cheeseman, J. R.; Montgomery, J. A., Jr.; Vreven, T.; Kudin, K. N.; Burant, J. C.; Millam, J. M.; Iyengar, S. S.; Tomasi, J.; Barone, V.; Mennucci, B.; Cossi, M.; Scalmani, G.; Rega, N.; Petersson, G. A.; Nakatsuji, H.; Hada, M.; Ehara, M.; Toyota, K.; Fukuda, R.; Hasegawa, J.; Ishida, M.; Nakajima, T.; Honda, Y.; Kitao, O.; Nakai, H.; Klene, M.; Li, X.; Knox, J. E.; Hratchian, H. P.; Cross, J. B.; Bakken, V.; Adamo, C.; Jaramillo, J.; Gomperts, R.; Stratmann, R. E.; Yazyev, O.; Austin, A. J.; Cammi, R.; Pomelli, C.; Ochterski, J. W.; Ayala, P. Y.; Morokuma, K.; Voth, G. A.; Salvador, P.; Dannenberg, J. J.; Zakrzewski, V. G.; Dapprich, S.; Daniels, A. D.; Strain, M. C.; Farkas, O.; Malick, D. K.; Rabuck, A. D.; Raghavachari, K.; Foresman, J. B.; Ortiz, J. V.; Cui, Q.; Baboul, A. G.; Clifford, S.; Cioslowski, J.; Stefanov, B. B.; Liu, G.; Liashenko, A.; Piskorz, P.; Komaromi, I.; Martin, R. L.; Fox, D. J.; Keith, T.; Al-Laham, M. A.; Peng, C. Y.; Nanayakkara, A.; Challacombe, M.; Gill, P. M. W.; Johnson, B.; Chen, W.; Wong, M. W.; Gonzalez, C.; Pople, J. A. *GAUSSIAN 03*, Revision C.02; Gaussian: Wallingford CT, 2003.
16. Krishnan, R.; Binkley, J. S.; Seeger, R.; Pople, J. A. *J. Chem. Phys.* **1980**, *72*, 650.
17. Wiberg, K. B. *J. Comput. Chem.* **2004**, *25*, 1342.
18. Reed, A. E. *J. Chem. Phys.* **1985**, *83*, 735; Reed, A. E.; Curtiss, L. A.; Weinhold, F. *Chem. Rev.* **1988**, *88*, 899.
19. Mulliken, R. S. *J. Chem. Phys.* **1955**, *23*, 1833; Mulliken, R. S. *J. Chem. Phys.* **1962**, *36*, 3428.
20. Gilli, G.; Bellucci, F.; Ferretti, V.; Bertolasi, V. *J. Am. Chem. Soc.* **1989**, *111*, 1023; Bertolasi, V.; Gilli, P.; Ferretti, V.; Gilli, G. *J. Am. Chem. Soc.* **1991**, *113*, 4917.
21. Gilli, P.; Bertolasi, V.; Ferretti, V.; Gilli, G. *J. Am. Chem. Soc.* **1994**, *116*, 909; Gilli, P.; Bertolasi, V.; Ferretti, V.; Gilli, G. *J. Am. Chem. Soc.* **2004**, *126*, 3845.
22. Gatti, C.; Cargnoni, F.; Bertini, L. *J. Comput. Chem.* **2003**, *24*, 422.
23. Grabowski, S. J.; Dubis, A. T.; Martynowski, D.; Glowka, M.; Palusiak, M.; Leszczynski, J. *J. Chem. Phys. A* **2004**, *108*, 5815.
24. Jensen, F. *Introduction to Computational Chemistry*; Wiley: New York, 1999.
25. Cramer, C. J. *Essentials of Computational Chemistry*; Wiley: New York, 2002.
26. Cioslowski, J. *Encyclopedia of Computational Chemistry*; Wiley: New York, 1988.
27. Krygowski, T. M. *J. Chem. Inf. Model* **1993**, *33*, 70.
28. Anslyn, E. V.; Dougherty, D. A. *Modern Physical Organic Chemistry*; University Science Books: California, 2004; p 1001.